

## Application of Modified Electrocoagulation for Efficient Color Removal from Synthetic Methylene Blue Wastewater

Xiaoxue Duan<sup>1</sup>, Pan Wu<sup>1</sup>, Kewu Pi<sup>1,2,\*</sup>, Huiqin Zhang<sup>1</sup>, Defu Liu<sup>1,2</sup>, Andrea R. Gerson<sup>3</sup>

<sup>1</sup> School of Resource and Environmental Engineering, Hubei University of Technology, Wuhan, Hubei 430068, China

<sup>2</sup> Hubei Key Laboratory of Ecological Restoration for River-Lakes and Algal Utilization, Wuhan, Hubei, 430068, China

<sup>3</sup> Blue Minerals Consultancy, Middleton, South Australia, 5213

\*E-mail: [pkw519@163.com](mailto:pkw519@163.com)

Received: 17 January 2018 / Accepted: 22 March 2018 / Published: 10 May 2018

---

Treatment of synthetic wastewater containing methylene blue (MB) by electrocoagulation with periodic electrode reversal (*PerevEC*) was evaluated. The Response Surface Methodology (RSM) procedure was employed to obtain optimal conditions for decolorization, electrode consumption and sludge production which were found to be cell voltage of 3.1 V, current density of 347 mA·cm<sup>-2</sup>, electrode reversal period of 2.5 s and inter-electrode gap of 2 cm. Under these conditions 97 ± 2 % of the color was removed, the electrode consumption and sludge production were 0.25 ± 0.02 kg(Al)·kg(MB<sub>r</sub>)<sup>-1</sup> (where kg(MB<sub>r</sub>)<sup>-1</sup> is per kg MB removed) and 1.9 ± 0.9 kg(sludge)·kg(MB<sub>r</sub>)<sup>-1</sup>, respectively. NMR, IR and SEM analyses of the precipitates, solutions and electrodes for *PerevEC* and traditional electrocoagulation without periodic reversal of the electrodes (*TradiEC*) show greater Al<sub>13</sub> Keggin ion polymer is formed in the electrolytic solution during *PerevEC*. Periodical reversal of the electrodes establishes improved conditions for precipitation and solution diffusion of Al<sup>3+</sup> with decreased anodic passivation and cathodic polarization. For both *PerevEC* and *TradiEC*, the disappearance of characteristic IR peaks at 800–890, 1350, 1490 and 1604 cm<sup>-1</sup> indicates the complete destruction of the methylene blue molecule by breakage of the central and side aromatic rings as well as demethylation. These results indicate that the *PerevEC* process, as compared to *TradiEC*, for dye wastewater treatment may be applied more widely due to the greater decolorization and reduced anodic passivation and cathodic polarization, although there is greater electrode consumption and sludge production.

---

**Keywords:** Electrochemical coagulation; Synthetic methylene blue wastewater; Periodical electrode reversal; Color removal, Response surface methodology

## 1. INTRODUCTION

Dyes are used extensively in textiles, printing, paper making, food processing and other industries, as well as everyday life. Consequently large quantities of dye-containing wastewater are produced throughout the world [1]. For instance, it has been reported that about 12% of synthetic dyes are used for textiles and of this 20% will be released into the ecosystem, with toxicity to microorganisms and humans [2]. Most of these dyes contain the structures of benzene ring and azo, which are resistant to degradation [3]. The major characteristics of many of the industrial dye wastewaters are high organic concentration, strong color, high-salt content and low biodegradability and removal rate [4, 5]. The release of dyes into water bodies is highly undesirable, resulting in reduced photosynthetic activity [6]. Accordingly, it is essential to develop effective methods for removal of color and toxicity prior to discharge.

Biological processes may be used for treatment of dye contaminated effluents but dyes tend to inhibit bacterial development [5]. Other processes, such as coagulation and adsorption [7, 8], photocatalytic degradation [2, 9, 10] and ozone oxidation [11, 12], micro-electrolysis [13, 14], advanced biological oxidation [8] and membrane separation technology [15, 16] have also been developed to treat this wastewater. However, these approaches have significant disadvantages, such as relatively high costs and the production of large amounts of enriched sewage mud [17].

Recently, because of its low price, reduced sludge production, availability, easy operation [18] and absence of additives, electrochemical coagulation has been found to be an effective method for treating waste water containing textile dyes [8, 19]. In addition, traditional electrocoagulation combined with other methods has been considered for increased decolorization. For instance, an electro/bio-oxidation combination for remediation of industrial azo-dyes wastewater [17] such as RB-5 dye [20], Yellow 160 azo dye [21]; assisted by Fenton for Acid Orange 7 removal [22]; coupled with kaolin for Acid Red 18 removal [23] and with phono- for triarylmethane dye removal [24] have also been reported.

However, the serious disadvantages of the traditional electrocoagulation process are cathodic polarization and anodic passivation which can hinder sustained and steady electrodisolution for further coagulation [19]. Hence, it is necessary to find alternative methods that are not only of low costs and high efficiency in removing dyes from wastewater but also have high current efficiency without electrode polarization and with less passivation. To the best of our knowledge there are few processes using electrochemical coagulation with periodic reversal of the electrodes (*PerevEC*) currently used to treat the wastewater containing textile dye wastewater. In our previous exploration [25], we concluded that *PerevEC* may have better prospects with regard to the efficiency and costs than conventional electrochemical coagulation for treating printing and dyeing wastewater containing methyl orange.

Methylene blue is also commonly used in industry. Consequently, electrochemical remediation of synthetic methylene blue wastewater has been studied widely [19]. Based on our previous study [25], the operating parameters for the treatment of synthetic wastewater containing methylene blue using *PerevEC* were investigated using the Response Surface Methodology (RSM) to achieve optimized color removal efficiency.

## 2. MATERIALS AND METHODS

### 2.1 Novel electrocoagulation

The Al<sub>13</sub> Keggin polymer is reported to play the greatest role in poly-aluminum coagulation [26, 27]. The formation of the Al<sub>13</sub> polymer is dependent on the total concentration of dissolved aluminum (for short, Al<sub>T</sub>) and other solution characteristics, e.g. pH and competitive ion concentrations [28]. For dyeing wastewater, color removal is a composite of the actions of Al<sub>13</sub> polymer and amorphous Al(OH)<sub>3</sub> [19, 29].

The concentrations of Al<sup>3+</sup>, OH<sup>-</sup> and Al(OH)<sub>4</sub><sup>-</sup> in the vicinity of the interfaces between the solution and the anode and/or cathode are much greater than those in the bulk of the solution particularly as the duration of electrolysis increases, which results in the concentration polarization [25]. Al(OH)<sub>4</sub><sup>-</sup> has been widely regarded as the main precursor for formation of the Al<sub>13</sub> Keggin polymer. Clearly, it is necessary to drive Al<sup>3+</sup> and OH<sup>-</sup> into the bulk solution for greater Al(OH)<sub>4</sub><sup>-</sup> formation [25]. In conventional electrolysis anodic passivation is a serious problem hindering further electrolysis as an oxide film is formed on the anode [19]. Consequently, reducing the formation of this oxide film could enable the continuous operation of electrocoagulation and enhance electrochemical efficiency.

Our previous research demonstrated that periodically reversing the electrodes may increase the transfer rate of Al<sup>3+</sup> and OH<sup>-</sup> into the bulk solution to form Al(OH)<sub>4</sub><sup>-</sup>, and thereafter to form Al<sub>13</sub> polymer. The current efficiency is enhanced and the cathodic polarization reduced [30, 31]. NaCl was used as the electrolyte since Cl<sup>-</sup> helps to destroy the metal oxide layer covering both electrodes [25], which helps to increase the anodic dissolution rate, resulting in greater release of aluminum hydroxide. This electrochemical technique provides an alternative indirect electro-oxidation method for the decolorization of dyeing wastewater with active chlorine species produced at the anode [32]. Greater removal rates are achievable with NaCl as the supporting electrolyte compared to other salts [18, 33]. For these reasons NaCl was used as the electrolyte in this to provide the desired current density values.

### 2.2 Electrocoagulation reactor

The electrocoagulation reactor employed in this study has been described previously [25]. This reactor can automatically reverse the role of the anode and cathode by a periodical reversal switch. The operational principle of this power supply was illustrated comprehensively in Pi et al. (2011), in which a rectangular voltage and zigzag current waveform was applied. The mechanisms and processes of electrocoagulation with or without periodic electrodes reversal (*PerevEC* or *TradiEC*) have also been illustrated [25, 31].

### 2.3 Electrocoagulation experiments

*PerevEC*: For each experiment, 500 mL of synthetic methylene blue wastewater was put into the reactor, and *PerevEC* was conducted for 30 min. After the electrocoagulation was finished, the

resultant suspension was settled for 30 min, followed by filtration of the wastewater through a 0.45  $\mu\text{m}$  pore membrane. The filtrate was assayed for the concentration of residual methylene blue. The mixture of the filtered residue and precipitate was centrifuged at 1000 rpm for 10 min, followed by drying at 105 °C for 2 h.

*TradiEC*: The traditional electrocoagulation process was also carried out in which all the experimental conditions for *PerevEC* were kept the same but without the periodic reversing of the electrodes.

#### 2.4 Analytical methods

The methylene blue (MB) concentration before and after electrocoagulation was assayed using UV/Vis spectroscopy (Shimadzu, Japan) with maximum absorbance at 664 nm [25, 34]. The solution pH value was adjusted with 1.0 M  $\text{H}_2\text{SO}_4$  or NaOH and was measured using a pH meter (Orion 210A, USA). Measurements for weight loss of the Al electrodes and weight of the dried solid mixture were used to calculate the electrode consumption (*ELC*) and the sludge production (*SP*) per kg MB removed [25]. NMR spectroscopic analysis (UNITY INOVA 600, Varian Inc., USA) was performed to confirm the existence and concentration of the  $\text{Al}_{13}$  Keggin polymers caused by hydrolyzation of the electrodissolved  $\text{Al}^{3+}$  solution. More detail can be found in our previous research [31] and Sheng et al [35]. IR spectra (NICOLET 5700 FTIR Spectrometer, USA) of the precipitates were collected using the KBr pellet (1:50) technique at 400–4000  $\text{cm}^{-1}$ . Scanning electron micrographs (JSM820 microscope, Japan) of the surface of the electrodes were obtained.

#### 2.5 Response Surface Methodology (RSM)

The RSM procedure was employed to optimize conditions to achieve maximum decolorization, *CR*, and minimum *ELC* and *SP*. The initial solution pH of 8.0 and MB concentration of 50  $\text{mg L}^{-1}$  were chosen according to our prior research [25]. The experimental parameters were current density (*j*), cell voltage (*U*), distance between electrodes (*d*), electrocoagulation time (*T*) and periodical electrode reversal time (*t*). The parameters and their ranges chosen for the RSM analyses, resulting from our previous studies, for treatment of MB wastewater are presented in Table 1. For the parameter variable analysis, 29 experiments were conducted for the evaluation of the combined effects amongst *U*, *j*, *d*, and *t* at the coded levels listed in Table 1.

**Table 1.** Levels and ranges of variables for *PerevEC* process.

Variables	Coded levels			+
	-1	0	1	
<i>U</i> (V)	3	4		5
<i>j</i> ( $\text{mA cm}^{-2}$ )	200	300	00	4
<i>d</i> (cm)	1	2		3
<i>t</i> (s)	1	2.5		4

### 3. RESULTS AND DISCUSSION

#### 3.1 Color removal efficiency (CR)

According to our previous results acquired for the *PerevEC* process, cathodic polarization can be impeded by applying an inter-electrode gap smaller than 4 cm [25]. Thus *PerevEC* measurements were conducted at  $d$  of 2.0 cm and  $T$  of 30 min. The variation of  $CR$  with respect to the operating parameters of  $j$ ,  $U$  and  $t$ , are given in **Figs. 1** and **2**. In **Fig. 1**  $t$  is held constant at 2.5 s. The optimum characteristics are defined as where the  $CR$  value is at the maximum or greater than 95%. As the solution current density was increased and the cell voltage decreased,  $CR$  increases (**Fig. 1**).

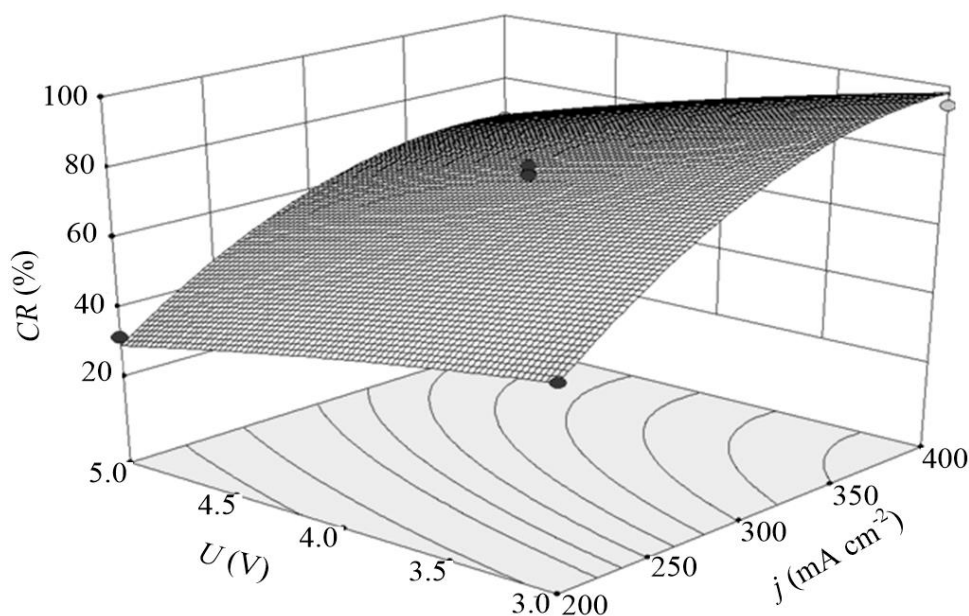


**Figure 1.** Effect of  $U$  and  $j$  on  $CR$  at  $d$  of 2.0 cm and  $t$  of 2.5 s, optimized by RSM.

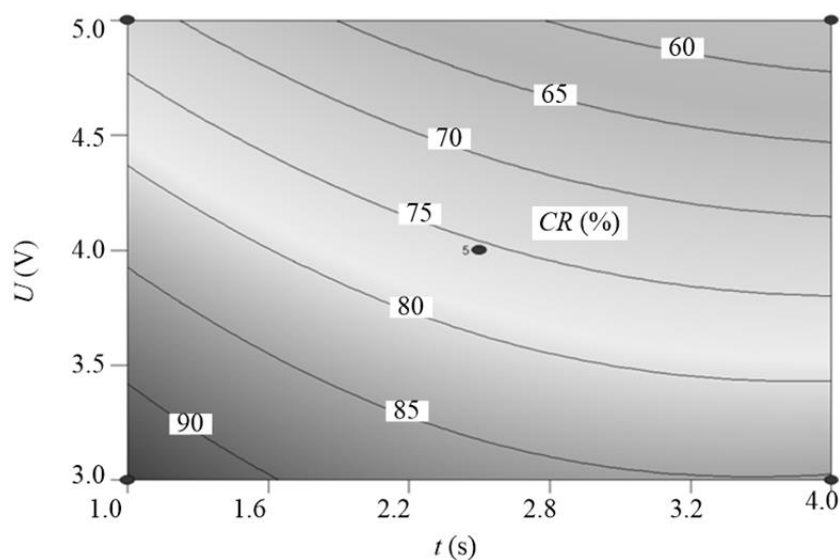


**Figure 2.** Effect of  $U$  and  $t$  on  $CR$  at  $d$  of 2.0 cm and  $j$  of 300 mA cm<sup>-2</sup>, optimized by RSM.

Current density ( $j$ ) has a significant effect on  $CR$ , and is positively correlated. With increasing current density, the solution conductivity and proton transfer rates increase. This results in more hydroxyl radicals ( $\text{OH}\cdot$ ) and aluminum ions being generated, which in turn results in greater generation of  $\text{Al}(\text{OH})_4^-$  and consequently the  $\text{Al}_{13}$  polymer [25]. The shorter the periodic electrode reversal time ( $t$ ), the smaller the anodic passivation and greater the production of aluminum ions, leading to greater decolorization efficiency.

### 3.2 Electrode consumption (ELC)

Electrode consumption is a very important parameter in determining economic performance of an electrocoagulation process [36, 37].  $ELC$  was measured at  $T$  of 30 min and  $U$  of 4.0 V. The variation of  $ELC$  with respect to the operating parameters,  $j$ ,  $d$  and  $t$  is shown in Figs. 3 and 4.

As  $j$  was increased from  $200 \text{ mA cm}^{-2}$ ,  $ELC$  decreased to its smallest value at  $346.9 \text{ mA cm}^{-2}$ , and then increased on further increase in current density to  $400 \text{ mA cm}^{-2}$  (Fig. 3). Increasing the inter-electrode distance resulted in a continuous decline in  $ELC$ . Over a short distance, although ion diffusion is suppressed, the small resistance between two adjacent electrodes results in high current density and commensurate aluminum precipitation rates. As the distance is increased, the rate at which the ions are produced slows as the adjacent solution resistance increases, corresponding to decreased electrode consumption. However, at low voltage and low current density, the electro-dissolved  $\text{Al}^{3+}$  are more likely to aggregate, resulting in greater floc formation [38]. The distance of 2 cm was found to be optimal for  $ELC$  consumption.

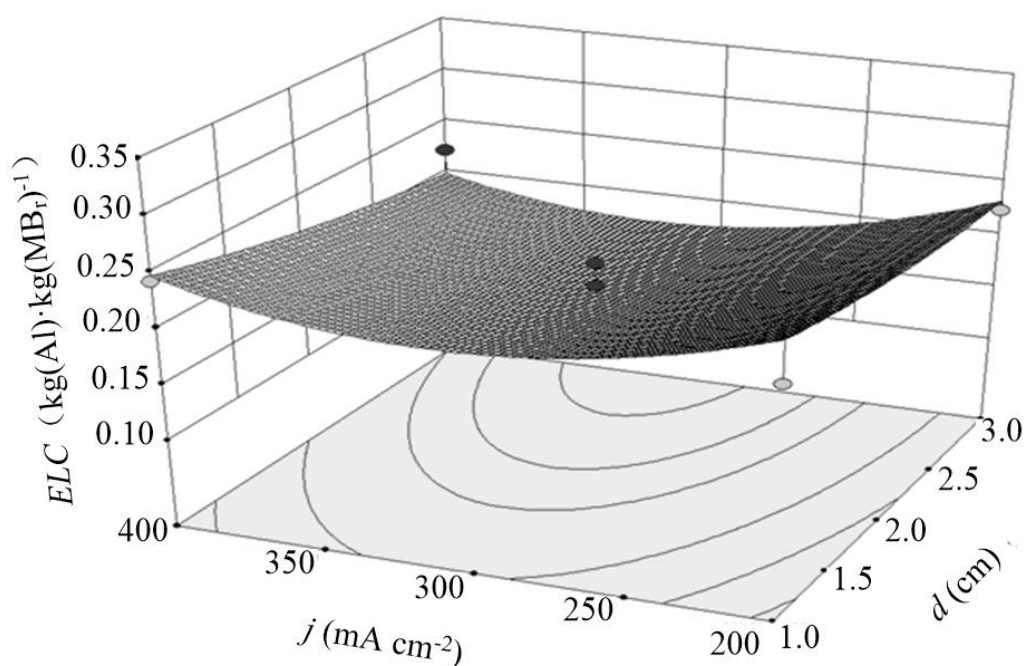


**Figure 3.** Effect of distance between electrodes ( $d$ ) and current density ( $j$ ) on  $ELC$  at  $t$  of 2.5 s and  $U$  of 4.0 V, optimized by RSM.

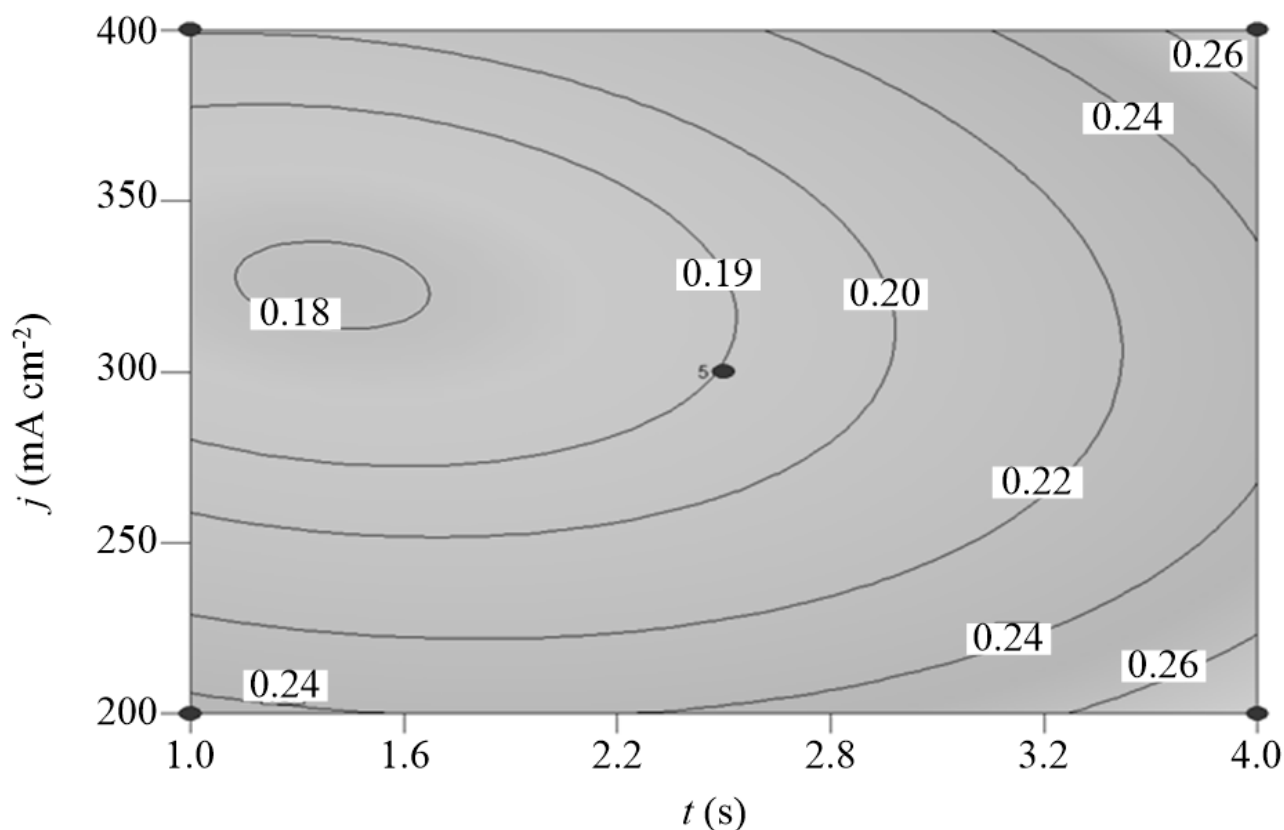


**Figure 4.** Effect of periodic electrode reversal time ( $t$ ) and current density ( $j$ ) on  $ELC$  at  $d$  of 2.0 cm and  $U$  of 4.0 V, optimized by RSM.

As can be seen from Fig. 4,  $ELC$  increases as the current density decreases and the electrode reversal time increases.  $0.22 \text{ kg(Al)} \cdot \text{g(MB}_t\text{)}^{-1}$  is consumed at  $i$  of  $220 \text{ mA cm}^{-2}$  for  $t$  of 1.6 s. To achieve the same  $ELC$  for the periodic cycle time of 2.5 s,  $i$  must be increased to  $400 \text{ mA cm}^{-2}$ . This may be mainly attributed to the retardation of the passivation layer formation on the anodic electrode with shorter reversal electrodes time [31].

Current densities in the range  $310\text{--}340 \text{ mA cm}^{-2}$  create improved conditions for blending the dye with flocs and result in reduced  $ELC$ . With current density greater than  $340 \text{ mA cm}^{-2}$  more energy is used in the production of  $\text{O}_2$  and heat generation, and byproducts generated from the electrodes increase rapidly [36]. This results in decreased energy efficiency for equivalent MB reduction.

### 3.3 Sludge production ( $SP$ )

Sludge production ( $SP$ ) is an essential index for evaluation of the environmental efficiency of electrochemical methods for dye wastewater remediation. Figs. 5 and 6 show the influence of  $j$ ,  $t$  and  $U$  at  $d$  of 2.0 cm on  $SP$ .

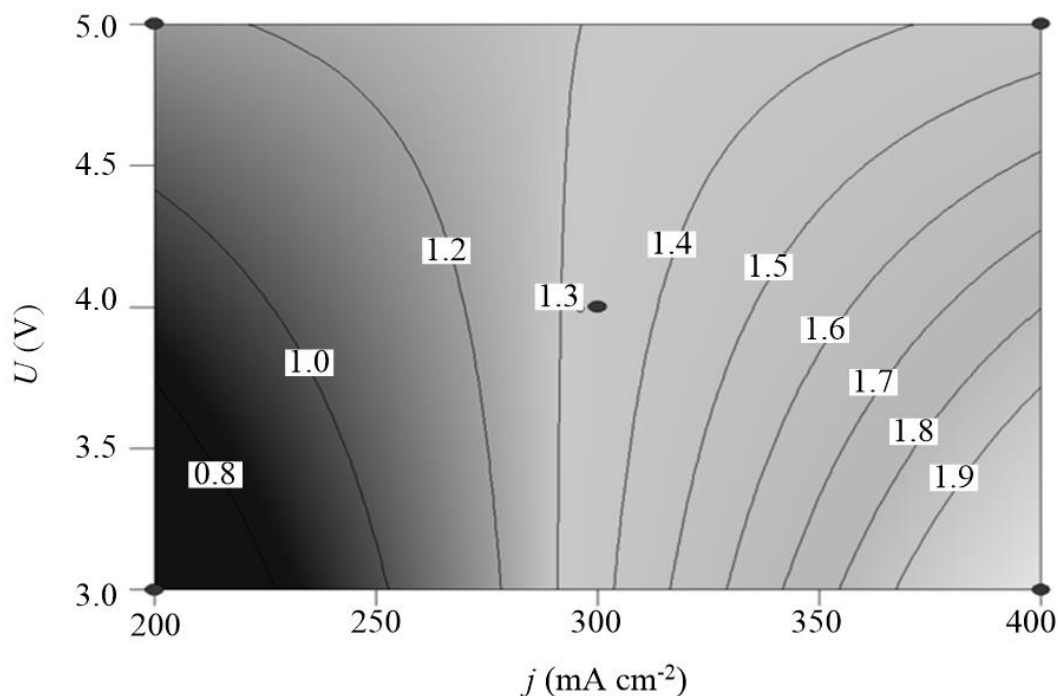


**Figure 5.** Effect of  $U$  and  $j$  on  $SP$  at  $d$  of 2.0 cm and  $t$  of 2.5 s.

In Fig. 5 the contour line is nearly parallel with the  $y$ -axis ( $U$ ) for current density of 300 mA  $\text{cm}^{-2}$  suggesting that cell voltage variation does not have significant effect on  $SP$  at this current density. For cell voltage of 4 V,  $SP$  increases from 0.9  $\text{kg}(\text{sludge}) \cdot \text{kg}(\text{MB}_r)^{-1}$  at  $j$  of 200 mA  $\text{cm}^{-2}$  to 1.3  $\text{kg}(\text{sludge}) \cdot \text{kg}(\text{MB}_r)^{-1}$  at  $j$  of 300 mA  $\text{cm}^{-2}$ . Further current density increase to 400 mA  $\text{cm}^{-2}$  results in 1.8  $\text{kg}(\text{sludge}) \cdot \text{kg}(\text{MB}_r)^{-1}$  at cell voltage of 4.0 V.

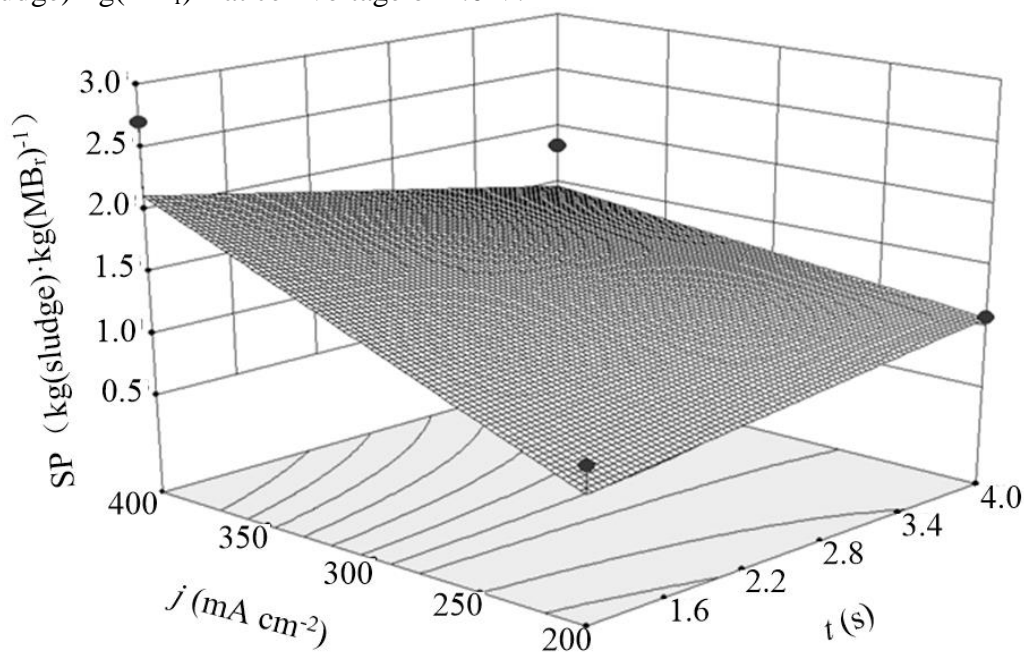


**Figure 6.** Effect of  $t$  and  $j$  on  $SP$  at  $U$  of 4.0 V and  $d$  of 2.0 cm.

As the current density increases, anode degradation increases as does *SP* [5]. However, at high current density, as the cell voltage is increased, the sludge production decreases. Increased cell voltage, in conjunction with excessive current density, results in generation of a large amount of bubbles at the anodic electrode [19, 31, 37]. These bubbles attach to the flocs making most of them float to the solution surface, resulting in many suspended flocs and little precipitate [25].

### 3.4 Validation of RSM optimal electrochemical operating parameters

Experimental parameters ( $U$ ,  $j$ ,  $t$ ,  $d$ ) for minimum *ELC* and *SP* and maximum *CR* have been confirmed using RSM (Figs. 1–6). These optimized parameters, as given by the Box-Behnken model of RSM, are  $U$  of 3.1 V,  $j$  of  $347 \text{ mA cm}^{-2}$ ,  $t$  of 2.5 s and  $d$  of 2.0 cm. Using these conditions, experiments were carried out for 90 min to examine the differences in *CR*, *ELC* and *SP*, between the values predicted by RSM and experimental values. These process conditions, using RSM, predicted *CR*, *ELC* and *SP* to be  $94 \pm 4 \%$ ,  $0.19 \pm 0.03 \text{ kg(Al)} \cdot \text{kg(MB}_r\text{)}^{-1}$  and  $1.7 \pm 0.1 \text{ kg (sludge)} \cdot \text{kg(MB}_r\text{)}^{-1}$ , respectively. The following experimental values were obtained:  $97 \pm 2 \%$ ,  $0.25 \pm 0.02 \text{ kg(Al)} \cdot \text{kg(MB}_r\text{)}^{-1}$ ,  $1.9 \pm 0.9 \text{ kg (sludge)} \cdot \text{kg(MB}_r\text{)}^{-1}$ . These results demonstrate that RSM is a suitable approach for optimizing experimental conditions for the treatment of dye wastewater containing methyl blue with maximum *CR* and minimised *ELC* and *SP*.

### 3.5 Comparison with *PerevEC* and *TradiEC*

Further experiments were conducted to compare differences in *CR*, *ELC*, and *SP*, between *PerevEC* and *TradiEC* at the optimized *PerevEC* conditions ( $U$  of 3.1 V,  $j$  of  $346.9 \text{ mA} \cdot \text{cm}^{-2}$ ,  $t$  of 2.5 s, and  $d$  of 2.0 cm).

Fig. 7 shows *CR* as a function of coagulation time for *TradiEC* and *PerevEC*. At 30 min *CR* using *PerevEC* was near to that of our previous exploration of methyl orange wastewater remediation [25], catalytic ozonation (ozone/activated carbon –  $\text{O}_3/\text{AC}$ )  $\text{O}_3$ -promoted traditional electrolysis with an removal efficiency 95.4 % for MB [39] and Bi-doped  $\text{TiO}_2$  photocatalytic oxidation for 60 min with 94.6 % efficiency [12]. As the electrocoagulation time was increased from 30 min to 90 min, *CR* increased steadily. *CR* for *TradiEC* and *PerevEC* increased from  $85 \pm 3 \%$  to  $91.0 \pm 0.5 \%$  and from  $94 \pm 2 \%$  to  $97.0 \pm 0.5 \%$ , respectively (Fig. 7a). These results are consistent with results reported by other researchers [38] that demonstrate that the process efficiency relates directly to the concentration of  $\text{OH}^-$  and  $\text{Al}^{3+}$  generated, as well as the subsequent concentration of flocs [19, 36]. These concentrations increase as the electrocoagulation time increases.

Compared with *PerevEC*, the *CR* of *TradiEC* increases more steadily with electrocoagulation time, showing that the current efficiency of *PerevEC* is greater than that of the *TradiEC* process. More of the voltage acts directly on electrode dissolution with less cathodic polarization and anodic passivation [31]. The electrode consumptions at 30–90 min for *PerevEC* and *TradiEC* were  $0.03\text{--}0.185 \text{ kg(Al)} \cdot \text{kg(MB}_r\text{)}^{-1}$  and  $0.02\text{--}0.06 \text{ kg(Al)} \cdot \text{kg(MB}_r\text{)}^{-1}$ , respectively (Fig. 7b).

Sludge production from both *PerevEC* and *TradiEC* increased with operating time as the anode dissolution increased. Although, the amount of sludge for *PerevEC* ( $1.47 \pm 0.5 \text{ kg(sludge)} \cdot \text{kg(MB}_r\text{)}^{-1}$ )

is greater than that for *TradiEC* ( $0.8 \pm 0.2 \text{ kg}(\text{sludge}) \cdot \text{kg}(\text{MB}_r)^{-1}$ ), greater MB removal is achieved using *PerevEC* than *TradiEC*. The sludge production of both *PerevEC* and *TradiEC* are much greater than those for methyl orange decolorization using electrocoagulation [25]. This is due to the differences in electrolysis time and current density applied to achieve optimum decolorization, which in turn is likely to be a function of the differences in molecular structure between methyl orange and blue. Decolorization not only depends on color adsorption and precipitation by chemical coagulation, but also the chromogen breaking from the benzene ring.

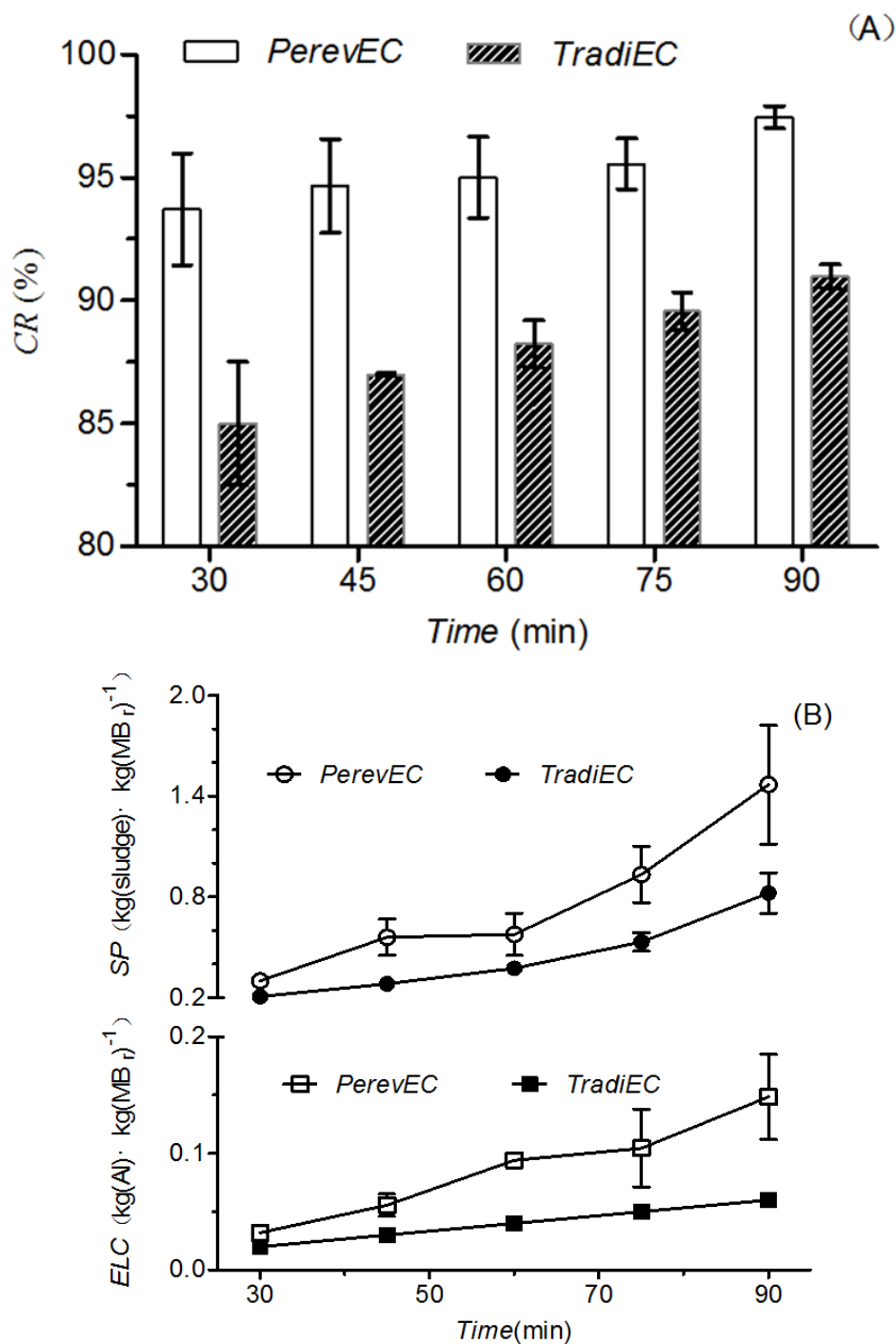
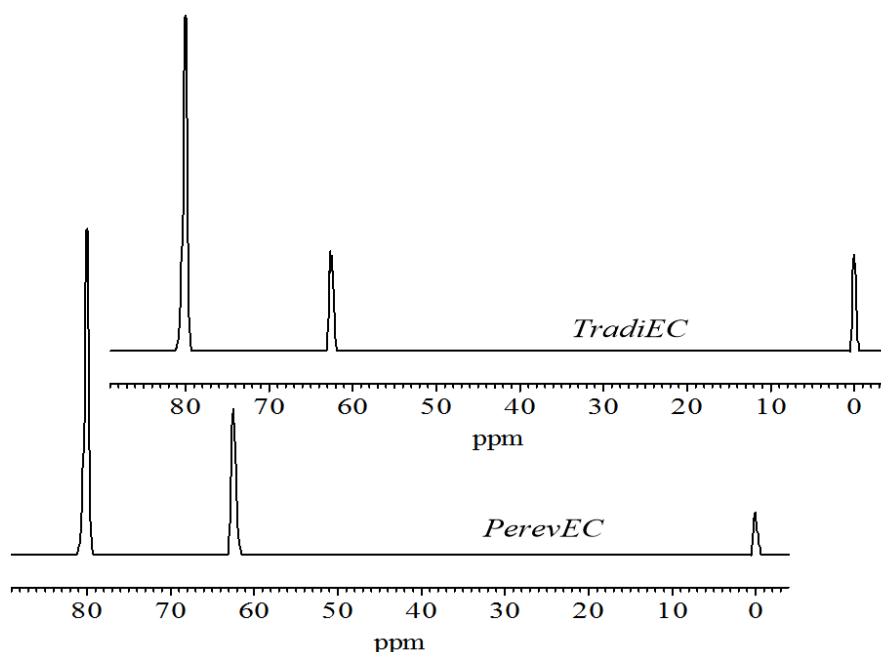


Figure 7. CR (A), ELC and SP (B) variation with electrocoagulation time for *PerevEC* and *TradiEC*.

Fig. 8 shows the  $^{27}\text{Al}$  NMR spectra of the resulting solutions formed by *PerevEC* and *TradiEC*. The intensity at 0 ppm resonance is proportional to the  $\text{Al}_a$  ( $[\text{Al}_2(\text{OH})_3]^{3+}$ ,  $[\text{Al}_5(\text{OH})_7]^{8+}$  and  $[\text{Al}_7(\text{OH})_3]^{18+}$ ) concentration in solution, and that at 63 ppm resonance represents the  $\text{Al}_{13}$  ( $([\text{AlO}_4\text{Al}_{12}(\text{OH})_{24}(\text{H}_2\text{O})_{12}]^{7+})$  polymer [28, 40]. The 80 ppm resonance is due to Na aluminate [35]. The content of  $\text{Al}_{13}$  polymer resulting from *PerevEC* is significantly greater than that from *TradiEC*. This results in an obvious increase in color removal due to *PerevEC* as compared to *TradiEC* as the  $\text{Al}_{13}$  polymer is the main active ingredient in the process of coagulation [28, 29, 41]. *PerevEC* results in the production of more  $\text{Al}^{3+}$  therefore resulting in greater concentration of the  $\text{Al}_{13}$  polymer and also enhances current efficiency by inhibiting cathodic polarization and anodic passivation [42].



**Figure 8.** NMR spectra of Al-containing species and precipitates caused by electrocoagulation due to *PerevEC* and *TradiEC*.

Fig. 9 shows the IR spectra of the original MB sample and the precipitates formed during *PerevEC* and *TradiEC*. The MB IR spectrum exhibits bands characteristic of the C=N central ring stretching vibration at  $1604\text{ cm}^{-1}$  [43] and C-S side ring stretching vibrations at  $1350\text{ cm}^{-1}$  and  $1490\text{ cm}^{-1}$  [44]. A wide and strong peak at  $3400\text{ cm}^{-1}$  can be seen due to the stretching vibration of -OH groups. The band due to C-H bending vibrations of various types ( $800\text{--}890\text{ cm}^{-1}$ ) is also apparent [44, 45].

After treatment by *PerevEC* and *TradiEC* IR spectra of the precipitates indicate that the ring stretching band at  $1604\text{ cm}^{-1}$  is shifted to  $1643\text{ cm}^{-1}$ , the ring stretching band at  $3400\text{ cm}^{-1}$  is shifted to  $3450\text{ cm}^{-1}$  and the symmetric C-N stretch at  $1395\text{ cm}^{-1}$  [46] is slightly shifted to  $1391\text{ cm}^{-1}$ . The characteristic bands of MB at  $800\text{--}890$ ,  $1350$ ,  $1490$  and  $1604\text{ cm}^{-1}$  are not visible indicating the destruction of the methylene blue molecule not only by demethylenation but also by breaking the side and central aromatic rings, resulting in destruction of the color producing groups (C-H, C-N, C-S) [43].

The precipitates from *PerevEC* and *TradiEC* give rise to almost same IR peaks indicating that the two methods have produced the same precipitate and may proceed via the same process mechanism.

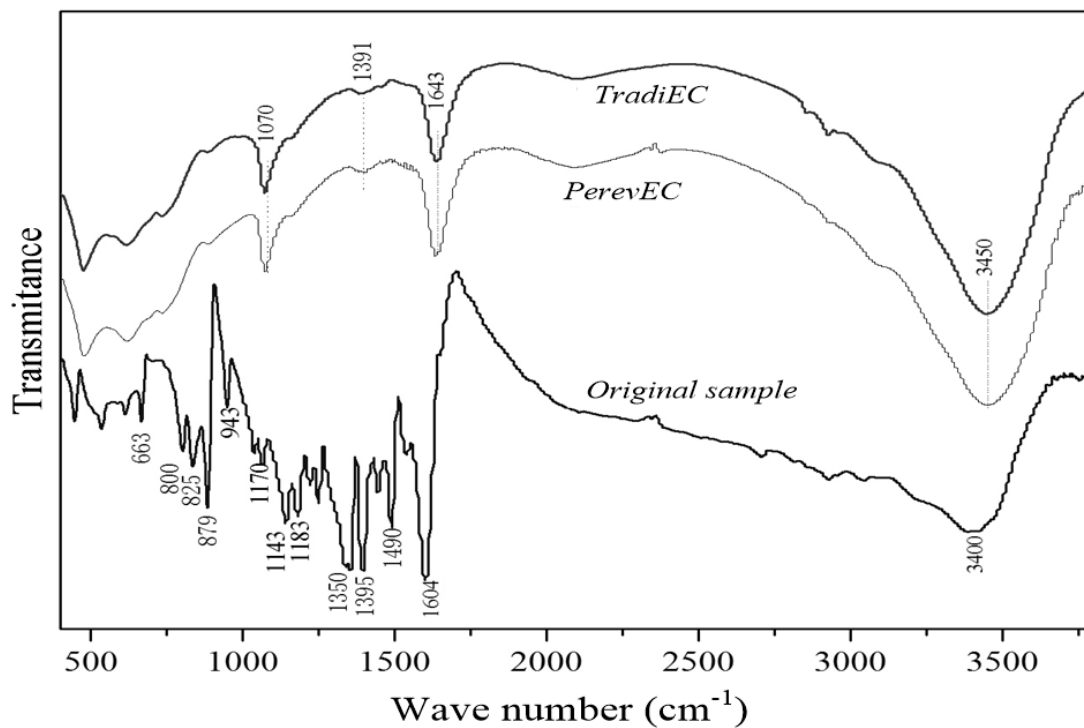


Figure 9. IR spectra of the precipitates of *PerevEC* and *TradiEC*.

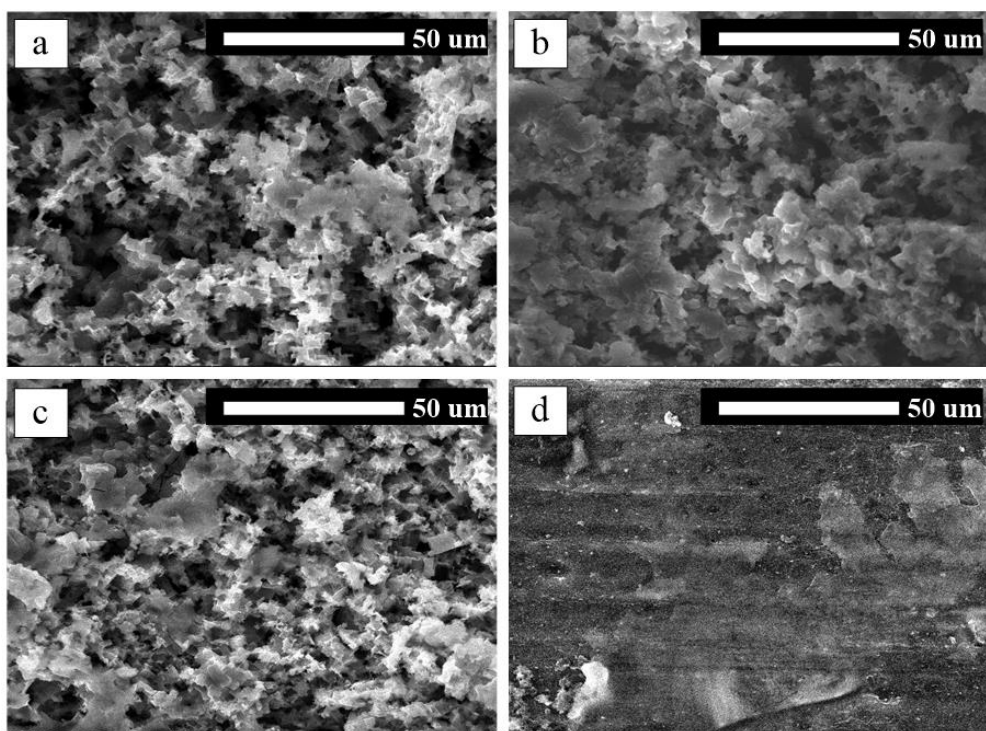


Figure 10. SEM images of the *PerevEC* electrodes (a and b) and *TradiEC* electrodes (c-anode, d-cathode).

To evaluate the structural features of the electrodes, a series of SEM micrographs were obtained. Figs. 10a, and b show parts of the electrode surfaces from *PerevEC* with irregularly large deep pits. Compared with *PerevEC*, the surface of *TradiEC* anodic electrode is more even and the pits are shallower (Fig. 10c). In contrast the surface of the *TradiEC* cathode (Fig. 10d) is flat, indicating that it either did not react or more likely that a surface film was formed through surface oxidation, which would result in reduced current efficiency and  $\text{Al}^{3+}$  dissolution rate.

#### 4. CONCLUSIONS

*PerevEC* was utilized to obtain optimal color removal efficiency (*CR*) and smaller sludge production (*SP*) and electrode consumption (*ELC*) for synthetic wastewater containing methylene blue dyes. Operating conditions optimized by the Box-Behnken model of RSM were cell voltage of 3.1 V, current density of  $347 \text{ mA}\cdot\text{cm}^{-2}$ , inter-electrode distance of 2.0 cm and time of periodically reversing electrodes of 2.5 s. Under these conditions, color removal was  $97 \pm 2 \%$ , with *ELC* and *SP* of  $0.25 \pm 0.02 \text{ kg(Al)}$  and  $1.9 \pm 0.9 \text{ kg(sludge)}$  for per kg methylene blue removal, respectively.

Compared with traditional electrocoagulation, electrocoagulation with periodic electrode reversal can effectively inhibit cathodic polarization and anodic passivation, and is considerably more effective at color removal of dye wastewater although there is greater electrode consumption and sludge production. Periodical electrode reversal provides favorable conditions for diffusion of the dissolved  $\text{Al}^{3+}$  ions, from the anode, which on reaction with  $\text{OH}^-$  ions form  $\text{Al}_{13}$ , resulting in more active electrocoagulation species.

#### ACKNOWLEDGEMENT

The authors would like to gratefully acknowledge the financial support from the National Natural Science Foundation of China ( Grant No. 91647207 ) .

#### References

1. L. Lin, Y. Lin, C. Li, D. Wu, H. Kong, *Int. J. Miner. Process.*, 148 (2016) 32-40.
2. M.H. Farzana, S. Meenakshi, *Appl. Catal. A-Gen.*, 503 (2015) 124-134.
3. Q. Lin, M. Gao, J. Chang, H. Ma, *Carbohydr. Polym.*, 151 (2016) 283-294.
4. S. Garcia-Segura, E. Brillas, *J. Photoch. Photobio. C.*, 31 (2017) 1-35.
5. A. Paz, J. Carballo, M.J. Pérez, J.M. Domínguez, *Chemosphere*, 181 (2017) 168-177.
6. G. Qian, L. Li, X. Hu, X. Yu, L. Ye, *Int. Biodeter. Biodegr.*, 125 (2017) 1-12.
7. B.C. Melo, F.A.A. Paulino, V.A. Cardoso, A.G.B. Pereira, A.R. Fajardo, F.H.A. Rodrigues, *Carbohydr. Polym.*, 181 (2018) 358-367.
8. C. R. Holkar, A. J. Jadhav, D. V. Pinjari, N. M. Mahamuni, A. B. Pandit, *J. environ. manage.*, 182 (2016) 351-366.
9. Q. Zhao, Z. Li, Q. Deng, L. Zhu, S. Luo, H. Li, *Electrochim. Acta*, 210 (2016) 38-44.
10. M.A. Hasnat, J.A. Safwan, M.S. Islam, Z. Rahman, M.R. Karim, T.J. Pirzada, A.J. Samed, M.M. Rahman, *J. Ind. Eng. Chem.*, 21 (2015) 787-791.
11. K.H. Hama Aziz, A. Mahyar, H. Miessner, S. Mueller, D. Kalass, D. Moeller, I. Khorshid, M.A.M. Rashid, *Process Saf. Environ.*, 113 (2018) 319-329.
12. M.S. Kumar, S.H. Sonawane, A.B. Pandit, *Chem. Eng. Process.*, 122 (2017) 288-295.

13. Y. Han, H. Li, M. Liu, Y. Sang, C. Liang, J. Chen, *Sep. Purif. Technol.*, 170 (2016) 241-247.
14. S. Zhang, D. Wang, L. Zhou, X. Zhang, P. Fan, X. Quan, *Chem. Eng. J.*, 217 (2013) 99-107.
15. J. Wang, Z. Wu, T. Li, J. Ye, L. Shen, Z. She, F. Liu, *Chem. Eng. J.*, 334 (2018) 579-586.
16. J. He, A. Cui, S. Deng, J.P. Chen, *J. Colloid Interf. Sci.*, 512 (2018) 190-197.
17. P. Aravind, H. Selvaraj, S. Ferro, M. Sundaram, *J. hazard. mater.*, 318 (2016) 203-215.
18. S. Aoudj, A. Khelifa, N. Drouiche, M. Hecini, H. Hamitouche, *Chem. Eng Process.*, 49 (2010) 1176-1182.
19. E. Brillas, C.A. Martínez-Huitle, *Appl. Catal. B-Environ.*, 166-167 (2015) 603-643.
20. V.M. Vasconcelos, C. Ponce-de-León, J.L. Nava, M.R.V. Lanza, *J. Electroanal. Chem.*, 765 (2016) 179-187.
21. A. Bedolla-Guzman, I. Sirés, A. Thiam, J.M. Peralta-Hernández, S. Gutiérrez-Granados, E. Brillas, *Electrochim. Acta*, 206 (2016) 307-316.
22. T.X.H. Le, T.V. Nguyen, Z.A. Yacoub, L. Zoungrana, F. Avril, E. Petit, J. Mendret, V. Bonniol, M. Bechelany, S. Lacour, G. Lesage, M. Cretin, *Chemosphere*, 161 (2016) 308-318.
23. Q. Zhuo, H. Ma, B. Wang, L. Gu, *J. hazard. mater.*, 142 (2007) 81-87.
24. C.H. Ng, C.A. Ohlin, B. Winther-Jensen, *Dyes. Pigments.*, 115 (2015) 96-101.
25. K.-W. Pi, Q. Xiao, H.-Q. Zhang, M. Xia, A.R. Gerson, *Process Saf. Environ.*, 92 (2014) 796-806.
26. W.-M. Zhang, J.-X. Zhuang, Q. Chen, S. Wang, W.-G. Song, L.-J. Wan, *Ind. Eng. Chem.*, 51 (2012) 11201-11206.
27. B. Zeboudji, N. Drouiche, H. Lounici, N. Mameri, N. Ghaffour, *Sep. Purif. Technol.*, 48 (2013) 1280-1288.
28. H.X. Tang, F. Xiao, D. Wang, *J. Colloid Interf. Sci.*, 226, Part A (2015) 78-85.
29. C. Hu, S. Wang, J. Sun, H. Liu, J. Qu, *Colloid. Surface. A.*, 489 (2016) 234-240.
30. K.W. Pi, W.Q. Gong, M. Wang, Z.Q. Huang, *Colloid. Surface. A.*, 330 (2008) 103-107.
31. K.W. Pi, L.X. Gao, Z. Li, M. Wang, L. Huang, *Colloid. Surface. A.*, 387 (2011) 113-117.
32. C.A. Martínez-Huitle, E. Brillas, *Appl. Catal. B-Environ.*, 87 (2009) 105-145.
33. W.-L. Chou, C.-T. Wang, S.-Y. Chang, *J. hazard. mater.*, 168 (2009) 1200-1207.
34. A.L. Webb, E.N. Taboada, L.B. Selinger, V.F. Boras, G.D. Inglis, *Water Res.*, 105 (2016) 291-296.
35. L. Sheng, Y. Zhang, F. Tang, S. Liu, *Micropor. Mesopor. Mat.*, 257 (2018) 9-18.
36. P. Asaithambi, B. Sajjadi, A.R. Abdul Aziz, W.M.A.B. Wan Daud, *Process Saf. Environ.*, 104, Part A (2016) 406-412.
37. A.K. Verma, *J. Water Process Eng.*, 20 (2017) 168-172.
38. H.J. Mansoorian, A.H. Mahvi, A.J. Jafari, *Sep. Purif. Technol.*, 135 (2014) 165-175.
39. J. Zhang, K.-H. Lee, L. Cui, T.-s. Jeong, *J. Ind. Eng. Chem.*, 15 (2009) 185-189.
40. B.L. Phillips, J.S. Vaughn, S. Smart, L. Pan, *J. Colloid Interf. Sci.*, 476 (2016) 230-239.
41. R. Li, B. Gao, K. Guo, Q. Yue, H. Zheng, Y. Wang, *Bioresource technol.*, 240 (2017) 59-67.
42. M. Paul, S.D. Jons, *Polymer*, 103 (2016) 417-456.
43. S.E.-d.H. Etaiw, M.M. El-bendary, *Appl. Catal. B-Environ.*, 126 (2012) 326-333.
44. O.V. Ovchinnikov, A.V. Evtukhova, T.S. Kondratenko, M.S. Smirnov, V.Y. Khokhlov, O.V. Erina, *Vib. Spectrosc.*, 86 (2016) 181-189.
45. P.H.B. Aoki, D. Volpati, W. Caetano, C.J.L. Constantino, *Vib. Spectrosc.*, 54 (2010) 93-102.
46. D. Zhang, L. Fu, L. Liao, N. Liu, B. Dai, C. Zhang, *Nano Res.*, 5 (2012) 875-887